MICROWAVE RADIOMETER INTER-CALIBRATION USING THE VICARIOUS CALIBRATION METHOD

Darren McKague
Chris Ruf
John J. Puckett

University of Michigan

ABSTRACT

The vicarious cold and warm calibration methods of Ruf, and Brown and Ruf, have been used to assess the calibration of the WindSat radiometer as well as the biases of the TMI, SSM/I F13 and SSM/I F14 radiometers relative to WindSat. WindSat biases computed as a function of scan position are consistent with a roll offset of the instrument of .2° and a pitch offset of .15°, and biases in the 6 GHz and 22 GHz channels of up to 8 Kelvins are consistent with an obstruction in the feed-horn edge of scan fields of view. Beam fractions and effective brightness temperatures of the obstructions are estimated for each affected channels using both the vicarious cold and warm calibration observations to produce an end-to-end WindSat calibration. Computed biases of TMI, SSM/I F13 and SSM/I F14 relative to WindSat agree well with independent estimates.

Index Terms— Microwave radiometry, Calibration

1. INTRODUCTION

If passive microwave data from multiple instruments are to be combined for use in, for example, the Global Precipitation Measurement (GPM) mission, the data must be well calibrated in an absolute sense and in a relative sense between instruments. That is, they must be well inter-calibrated, with the absolute and relative calibrations connected via some common reference. To function properly, the details of the calibration process and comparison to a common reference must be well understood. That is the goal of the GPM Inter-Calibration Working Group (ICWG). This paper focuses on one particular method, the vicarious calibration method applied to both the cold end of the measurement range (Section 2) and the warm end of the measurement range (Section 3), and end-to-end calibration using both (Section 4). The results shown are averages over data from July 2005 through June 2006 for the WindSat, Tropical Rainfall Measurement Mission Microwave Imager (TMI), and two versions of the Special Sensor Microwave Imager (SSM/I) on board the F13 and F14 satellites.

2. VICARIOUS COLD CALIBRATION

Data for the radiometers in question have been analyzed using vicarious cold calibration [1]. For relative calibration between radiometers, WindSat is used because of its combination of global coverage and range of channels.

Before comparing WindSat data to the other radiometers, an analysis is performed to determine WindSat scan position dependent biases. For this, WindSat vicarious cold brightness temperatures as a function of scan position are compared to the center of scan. The mean for the 10 center scan positions is used as the reference here and for comparisons with other radiometers. Two significant features are evident: large edge of scan biases in the 6 GHz and 22 GHz data, and a polarization dependent slope in the cross scan bias. The edge of scan biases are believed to be due to obstructions, such as the external warm and cold loads, which enter the respective feed-horn field of view at either end of the Earth viewing portion of the WindSat scan [2]. Section 4 will discuss this bias further. The polarization dependent slope is consistent with attitude offsets in the instrument.

For the scan position dependent bias slope, the magnitude is larger, and opposite in sign, for the vertical polarization (V-pol) relative to horizontal (H-pol). Over ocean brightness temperatures, and hence the vicarious cold brightness temperatures, are sensitive to small changes in Earth incidence angle (EIA) [1]. This sensitivity is higher, and opposite in sign, for V-pol than for H-pol. EIA will vary as a function of scan position from its nominal value for any roll or pitch attitude offset in the instrument in a systematic manner that can be readily modeled [3]. Given such a model and a model of the effect of EIA on ocean brightness temperatures [4], observed scan position dependent biases can be used to assess attitude offsets in the instrument. The WindSat cold calibration biases shown in Figure 1 are consistent with an instrument roll offset of .2° and a pitch offset of .15°. With these attitude corrections, the WindSat data are a more accurate reference for inter-calibration.

The vicarious cold biases for TMI, SSM/I F13 and SSM/I F14 relative to WindSat center of scan as a function of scan position are shown in Figures 2, 3, and 4. The method of Brown et al. [5] was used with Global Data Assimilation System (GDAS) data and the ocean surface emissivity model of Elsaesser and Kummerow [4] for calculating theoretical vicarious cold brightness temperatures. For both SSM/I instruments, an offset in these biases consistent with an offset from the nominal EIA is seen. Figure 5 shows the cold calibration data with an EIA correction of -.15° for F13 and -.08° for F14. For both instruments, the 19 GHz V-pol and H-pol and 37 H-pol channel biases reduce to near zero with this correction. Significant biases relative to WindSat remain in the other SSM/I channels and in all of the TMI channels. The sources of these biases are outside the scope of this paper.

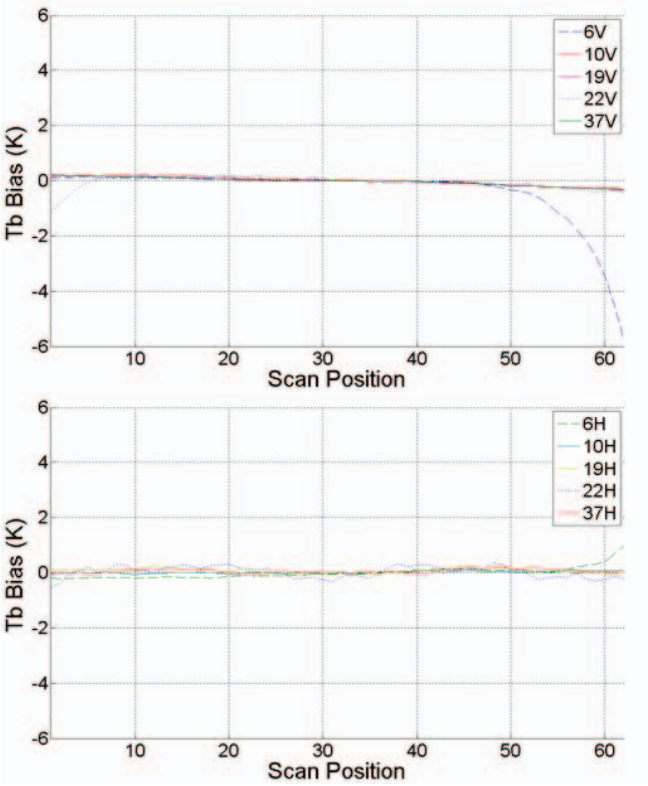

Figure 1. WindSat vicarious cold biases relative to center of scan. Vertical polarization channels are on top, horizontal polarization channels are on bottom. These biases are consistent with a roll offset of .2° and a pitch offset of .15°.

Table 1 shows vicarious cold biases for TMI relative to WindSat. The biases from Hong et al. [6] are shown for comparison, though the data are from a different period. Also shown in Table 1 are the biases with corrections for EIA offsets from nominal, as well as the vicarious warm biases which are described in Section 3. Table 2 shows the same data for SSM/I F13 and F14. Note the similarity in biases relative to WindSat for these two instruments, and the removal of the 19 GHz and 37 GHz horizontal channel biases with the correction for EIA offsets.

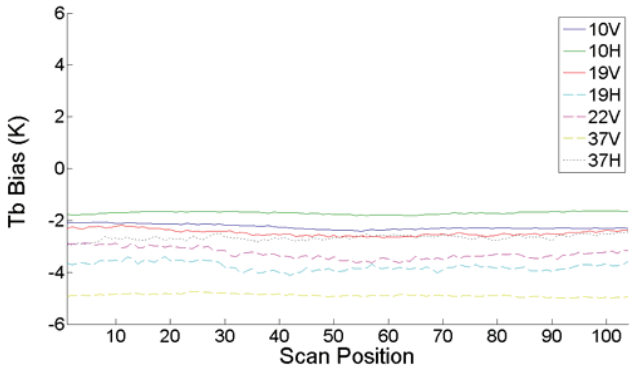

Figure 2. TMI cross scan biases relative to WindSat center of scan.

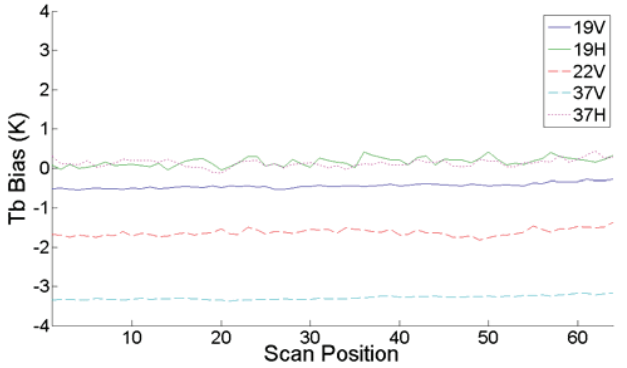

Figure 3. SSM/I F13 cross scan biases relative to WindSat center of scan.

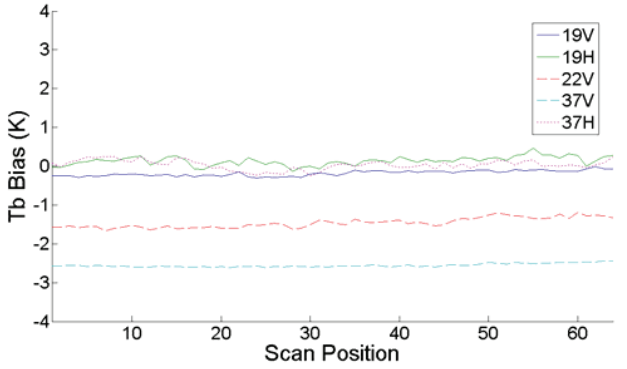

Figure 4. SSM/I F14 cross scan biases relative to WindSat center of scan.

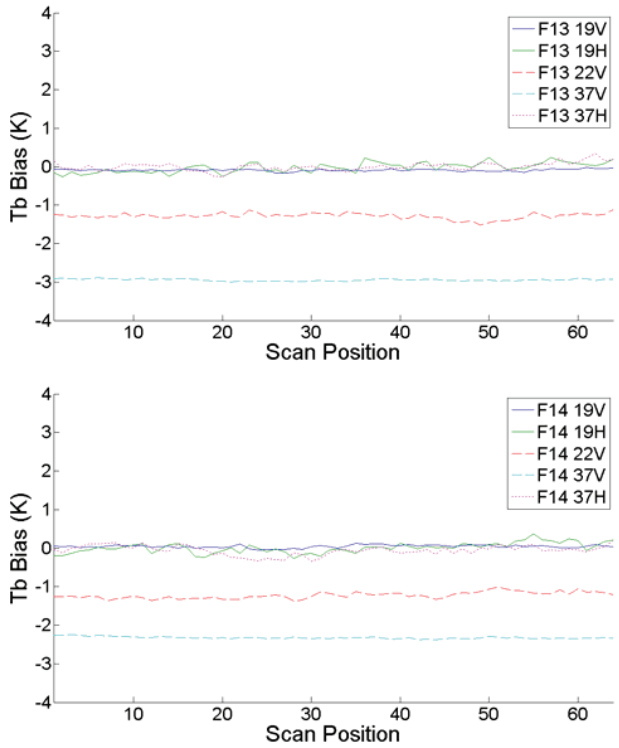

Figure 5. SSM/I F13 and F14 cross scan biases relative to WindSat with an EIA offset of -.15° and -.08° respectively.

Table 1. Average TMI biases relative to WindSat. Results from Hong et al. [6] are shown for comparison.

	Channel						
	10V	10H	19V	19H	22V	37V	37H
Cold Biases Nominal EIA	-1.8	-1.5	-2.5	-3.4	-2.5	-4.6	-2.6
Cold Biases Hong et al., "All"	-1.1	-1.7	-2.3	-2.3	-3.1	-4.0	-2.3
Cold Biases EIA corrected	-1.6	-1.7	-2.2	-3.6	-2.2	-4.2	-2.8
Warm Biases	-0.5	-0.5	-0.6	-1.0	-2.5	-2.6	-2.5
Warm Biases Wilheit	-0.8	-0.5	-0.5	-1.1	-2.8	-2.7	-2.6

Table 2. Same as Table 1, but for SSM/I F13 and F14.

	Channel Biases Relative to WindSat (K)				
	19 V	19 H	22 V	37 V	37H
F13 Cold Nominal EIA	-0.4	0.3	-1.6	-3.3	0.1
F13 Cold Corrected EIA	-0.1	0.0	-1.3	-2.9	0.0
F14 Cold Nominal EIA	-0.2	0.1	-1.5	-2.6	0.0
F14 Cold Corrected EIA	0.0	0.0	-1.2	-2.3	-0.1
F13 Warm	-0.4	-0.8	-1.0	-2.0	-2.0
F14 Warm	-0.5	-0.9	-1.2	-1.9	-1.6

3. VICARIOUS WARM CALIBRATION

As with the vicarious cold calibration, the data have been analyzed using the vicarious warm calibration method of Brown and Ruf [7] using GDAS data to model the atmospheric contribution to the measured brightness temperatures. The vicarious warm biases for WindSat relative to center of scan as a function of scan position are shown in Figure 6. Since the vicarious warm observations are made over land, the sensitivity to EIA, and hence to attitude offsets, is negligible. However, the obstruction at the edge of scan for 6 GHz and 22 GHz channels has increased to as much as 8 Kelvins.

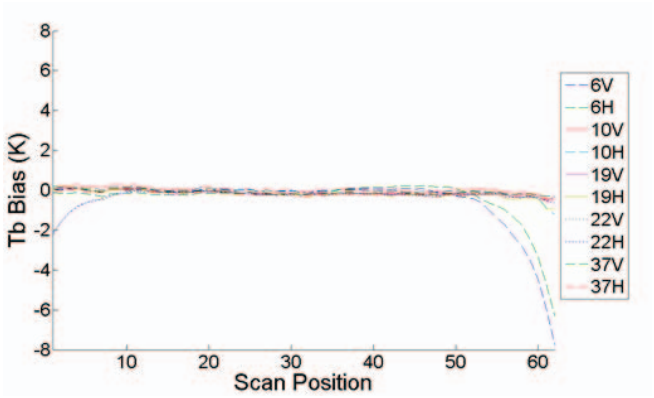

Figure 6. WindSat vicarious warm biases relative to scan center as a function of scan position.

The vicarious warm biases for TMI, SSM/I F13 and SSM/I F14 relative to WindSat center of scan are given in Tables 1 and 2. For comparison, independent estimates of the warm end TMI, WindSat relative biases from Wilheit [8] are shown in Table 1.

4. END-TO-END CALIBRATION AND EDGE OF SCAN OBSTRUCTIONS

As mentioned above, the edge of scan biases seen on WindSat are believed to be due to obstructions emitting and scattering radiation into the feed horn fields of view. We can describe this mathematically with the equation:

$$T_A = T_{b,mb} * (1 - bf_{sl}) + T_{b,obst} * bf_{obst} \qquad (1)$$

where T_A is the measured antenna temperature, $T_{b,mb}$ is the main beam brightness temperature, $T_{b,obst}$ is the effective radiating temperature of the obstructions, and bf_{obst} is the beam fraction intercepted by the obstructions. Estimating $T_{b,obst}$ and bf_{obst} requires observations of T_A with know $T_{b,mb}$; these are taken from the vicarious cold and vicarious warm calibration data. From the vicarious calibration observations, $T_{b,mb}$ is estimated at the edge of scan from the center of scan vicarious brightness temperatures with

corrections for instrument attitude offsets as described above. Since the beam patterns change from channel to channel, separate estimates of $T_{b,obst}$ and bf_{obst} are made for each channel. It is assumed that $T_{b,obst}$ is the same for all edge of scan positions for a given channel and that only bf_{obst} varies with scan position. Results are shown in Figure 7 and Table 3. WindSat vicarious cold biases with both EIA and edge of scan interference corrections are shown in Figure 8.

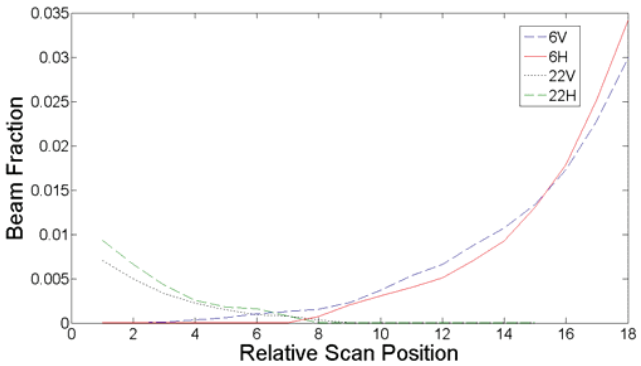

Figure 7. Edge of scan obstruction beam fractions as a function of relative scan position from beginning (22 GHz) or end (6 GHz) of the WindSat scan.

Table 3. Edge of scan obstruction effective brightness temperatures for WindSat.

Channel	Side-lobe Effective T_b (K)
6V	2.7
6H	94.4
22V	2.7
22H	78.2

5. CONCLUSIONS

The vicarious cold and vicarious warm calibration methods have been used to assess scan position dependent biases in WindSat data as well as the calibration of WindSat relative to TMI, SSM/I F13 and SSM/I F14. The scan position dependent biases in WindSat are consistent with a pitch and roll attitude offset of the WindSat instrument. WindSat shows significant edge of scan biases at 6 GHz and 22 GHz. Using both the vicarious cold and warm calibration data, estimates of the effective brightness temperatures and beam fractions of the edge of scan interferers creating these biases have been made. Biases of WindSat relative to TMI are consistent with independent estimates for both warm and cold calibration. Relative biases between WindSat and both SSM/I instruments are similar and are consistent with EIA offsets in both SSM/Is. Future work will focus on determining the sources of remaining relative biases in these calibration data as well as determining attitude offsets in the TMI instrument form the vicarious cold calibration data and characterizing the uncertainties in the edge of scan obstruction analysis.

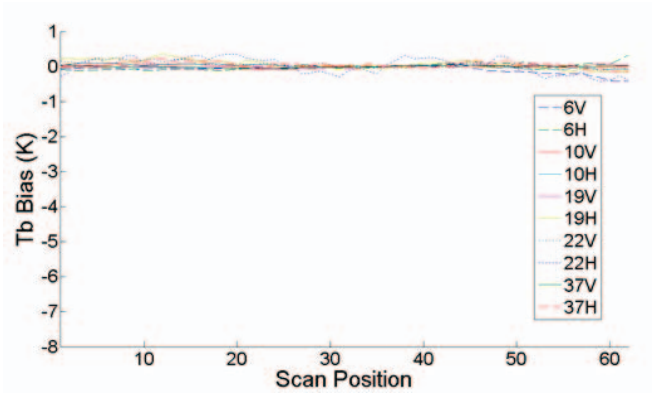

Figure 8. WindSat vicarious cold biases relative to center of scan with EIA and edge of scan bias corrections.

5. ACKNOWLEDGEMENT

The work presented here was funded in part by NASA grant NNX07AD69G.

11. REFERENCES

[1] Ruf, C.S. "Detection of calibration drifts in spaceborne microwave radiometers using a vicarious cold reference," *IEEE Trans. Geosci. Remote Sens.*, **38**(1), 44-52, 2000.

[2] Bettenhausen, Michael H., Elizabeth Twarog and Peter Gaiser, "On-Orbit Calibration of WindSat Brightness Temperatures," *Proc. IEEE International Geoscience and Remote Sensing Symposium*, Barcelona, Spain, July 23-27, 2007.

[3] Wentz, F. J., "Sensor Calibration and Ocean Products for TRMM Microwave Radiometer, Final Progress Report," *NASA Technical Report*, 2003.

[4] Elsaesser, G. S. and C. K. Kummerow, "Towards a fully parametric retrieval of the non-raining parameters over the global oceans," *J. Appl. Meteor. & Climatol.*, 2007.

[5] Brown, S., C. Ruf, S. Keihm and A. Kitiyakara, "Jason Microwave Radiometer performance and on-orbit calibration," *Marine Geodesy*, **27**(1-2), 199-220, 2004.

[6] Hong, Liang, W. L. Jones, and T. T. Wilheit, "Inter-satellite Radiometer Calibrations between WindSat, TMI and AMSR," *Proc. IEEE International Geoscience and Remote Sensing Symposium*, Barcelona, Spain, July 23-27, 2007.

[7] Brown, S., and C. Ruf, "Determination of a Hot Blackbody Reference Target over the Amazon Rainforest for the On-orbit Calibration of Microwave Radiometers," *AMS J. Oceanic Atmos. Tech.*, **22**(9), 1340-1352, 2005.

[8] Wilheit, T., personal communication, April 2009.